2008 American Control Conference
Westin Seattle Hotel, Seattle, Washington, USA
June 11-13, 2008

Model and Experimental Validation of a Controllable Membrane-Type Humidifier for Fuel Cell Applications

Denise A. McKay, Anna G. Stefanopoulou, and Jeffrey Cook
Fuel Cell Control Laboratory, University of Michigan, Ann Arbor, MI, USA

Abstract— **For temperature and humidity control of fuel cell reactants, a gas humidification apparatus was designed and constructed. We then developed a low-order, control-oriented model of the humidification system thermal dynamics based on first principles. A simple and reproducible methodology is then employed for parameterizing the humidification system model using experimental data. Finally, the system model is experimentally validated under a wide range of operating conditions. It is shown that a physics based estimation of the air-vapor mixture relative humidity leaving the humidifier system (supplied to the fuel cell) is possible using temperature and pressure measurements. This estimation eliminates the need for a bulky and expensive humidity sensor and enables the future application of temperature feedback control for thermal and humidity management of the fuel cell reactants.**

I. INTRODUCTION

Polymer electrolyte membrane fuel cells operate at low temperature sufficient for fast startup [1], and are considered as viable power generators for automotive applications. To maintain high membrane conductivity and durability, the supplied reactants (hydrogen and oxygen from the air) require humidification. However, excess water can condense and affect fuel cell performance [2], requiring accurate and fast control of the gas humidity supplied to the fuel cell [3].

Several humidification strategies have been considered for fuel cell reactant pre-treatment, including bubblers and spargers [4]. However, the relatively compact, light weight and fast thermal response of membrane-type humidifiers have gained increased attention. A membrane humidifier, shown in Fig. 1, directs dry gas across one surface of a polymeric membrane and hot liquid water (or a hot gas saturated with water vapor) across the other surface. Water vapor and thermal energy are exchanged through the membrane, from the liquid water to the dry gas, to heat and humidify the gas.

Typically, membrane humidifiers are internal to the fuel cell and direct coolant water (or humidified fuel cell exhaust gas) from the power producing portion of the fuel cell to the humidifier to heat and humidify the supplied gas [2], [5], [6]. These humidifiers are designed to saturate a gas at the temperature of the coolant exiting the fuel cell. While compact, these internal humidifiers prohibit active humidity regulation and couple reactant humidity requirements to the fuel cell cooling demands. To overcome the humidity constraints, sliding plates were considered to activate and deactivate gas channels within the humidifier to control the contact area between the liquid and gas [7].

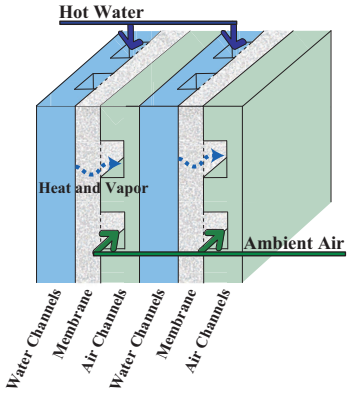

Fig. 1. Schematic diagram of a 2-cell membrane based humidifier.

The humidification system considered here decouples the passive humidifier from the fuel cell cooling loop and employs a gas bypass for humidity control, similar to [8]. To design adequate controllers for thermal regulation (using heaters) and humidity control (for the gas flow split between the humidifier and bypass), we developed a low order model based on first principles. Similar to engine thermal management systems employing either a valve or servo motor to bypass coolant around a heat exchanger [9], [10], the coordination of the heaters and bypass is challenging during fast transients due to the different time scales, actuator constraints, and sensor responsiveness. An additional complexity arises from the need to avoid condensation due to system disturbances. The low-order control-oriented model developed here will enable systematic controller tuning of the multiple interconnected thermal loops, better sizing of the actuators (heaters), and sensor selection and placement.

II. HARDWARE AND SYSTEM OPERATION

The humidification system hardware[1] was installed in the Fuel Cell Control Laboratory at the University of Michigan. The system was designed to deliver moist air at 45^o-65^{o}C and 50%-100% relative humidity at dry air mass flow rates up to 40 slm, corresponding to 300% excess oxygen in the cathode of a 0.5 kW fuel cell.

The humidification system consists of five control volumes, namely the water heater, humidifier, reservoir, bypass,

This work is funded by the U.S. Army Center of Excellence for Automotive Research (DAAE07-98-3-0022) and the National Science Foundation (CMS 0625610).

Corresponding author e-mail address: dmckay@umich.edu

[1]Designed in collaboration with the Schatz Energy Research Center at Humboldt State University

and mixer. Fig. 2 shows the interaction of the air and liquid water as they move through these control volumes, where the letter M in (kg/mol) is used to denote molar mass, P in (Pa) for pressure, Q in (W) for heat added to a control volume, r for the fraction of the total air flow, T in (K) for temperature, W in (kg/s) for mass flow rate, and the symbol ϕ for relative humidity. Subscripts are used to indicate first the substance of interest, where a is for air, b for bulk materials, g for gas mixture, l for liquid water and v for water vapor; secondly the control volume such as bp for bypass, cv generically for control volume, r for reservoir, fc for fuel cell, wh for water heater, hm for humidifier, and mx for mixer; finally an i or o indicates the control volume inlet or outlet.

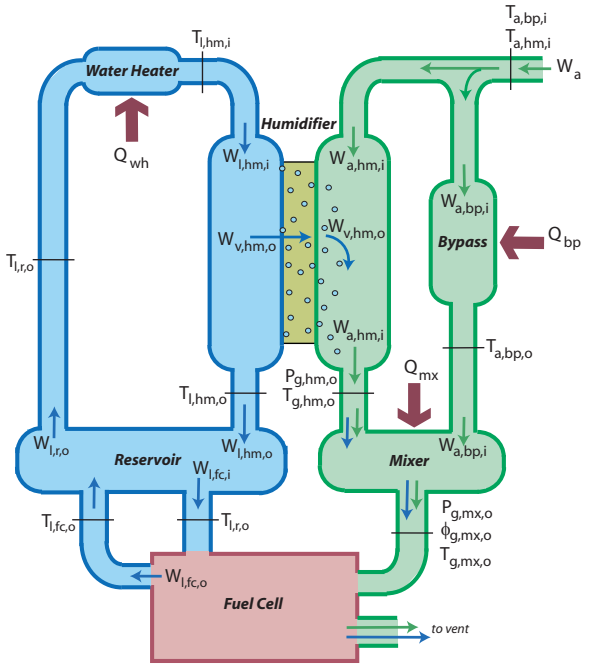

Fig. 2. Controllable humidification system indicating states, disturbances and measurements. Thin arrows represent mass flow directions and large thick arrows indicate locations where control action is applied.

When the humidifier system is coupled with a fuel cell, the total mass flow of dry air through the system, W_a, is a function of the amount of current produced by the fuel cell and can be thought of as a disturbance while the fraction of the air that is supplied to the bypass, r_{bp}, or humidifier, r_{hm}, is controlled with mass flow controllers regulating the bypass and humidifier air mass flow rates, $W_{a,bp,i}$, and $W_{a,hm,i}$. The number of cells in the humidifier, as well as the membrane surface aera, were chosen to ensure that the humidifier produces a saturated air stream at a temperature, $T_{g,hm,o}$, dependent upon the supplied liquid water temperature, $T_{l,hm,i}$. The air bypassing the humidifier is heated, with a 50W resistive heater, Q_{bp}. The saturated air stream from the humidifier and the dry air stream from the bypass are combined in the mixer to produce a desired air-vapor mixture relative humidity, $\phi_{g,mx,o}$, to be supplied to the fuel cell. A 52W resistive heater, Q_{mx}, is used in the mixer for temperature control and to minimize condensation during the mixing of the saturated and dry gases.

Liquid water is circulated from the reservoir through the water heater and humidifier using a pump and manual throttle valve for controlling the liquid water flow rate. The water reservoir is shared with the fuel cell coolant loop, containing a heat exchanger, fan and circulation pump which are not shown. Liquid water from the fuel cell is an input to the reservoir at the fuel cell coolant temperature, $T_{l,fc,o}$. To mitigate reservoir thermal disturbances and offset heat losses to the ambient, a 1000W resistive heater, Q_{wh}, is used to heat the liquid water before entering the humidifier.

III. RELATIVE HUMIDITY OUTPUT ESTIMATION

The relative humidity of the air supplied to the fuel cell from the mixer, considered as a system output, must be known to ensure adequate controller performance. However, humidity sensors, although responsive and accurate for laboratory measurements, are prohibitively expensive and bulky for commercial applications. As a result, a relative humidity estimator is constructed and compared to a relative humidity measurement with an accuracy of 1.5%.

First, the mass flow rate of water vapor leaving the humidifier is assumed equal to that leaving the mixer, $W_{v,hm,o} = W_{v,mx,o}$. Applying the definition for the humidity ratio, $\omega = \frac{M_v \phi P^{sat}}{M_a(P-\phi P^{sat})}$, the water vapor mass flow rate exiting a control volume is generally described by

$$W_{v,cv,o} = \frac{M_v \phi_{g,cv,o} P^{sat}_{g,cv,o}}{M_a(P_{g,cv,o} - \phi_{g,cv,o} P^{sat}_{g,cv,o})} W_{a,cv,o} \ . \qquad (1)$$

The air mass flow rates entering and exiting the mixer are assumed equal, implying W_a=$W_{a,hm,i}$+$W_{a,bp,i}$. Substituting the air mass continuity equation into the water mass continuity equation, and applying the water vapor mass flow rate definition from (1), the mixer outlet relative humidity is:

$$\phi_{g,mx,o} = \phi_{g,hm,o} r_{hm} \frac{P^{sat}_{g,hm,o}}{P^{sat}_{g,mx,o}} \left(\frac{P_{g,mx,o}}{P_{g,hm,o} - r_{bp}\ \phi_{g,hm,o}\ P^{sat}_{g,hm,o}} \right) , \qquad (2)$$

where $r_{bp} = W_{a,bp,i}/W_a$, $r_{hm} = W_{a,hm,i}/W_a$, and $P^{sat}_{g,hm,o}$ and $P^{sat}_{g,mx,o}$ are the water vapor saturation pressures (evaluated at the temperature location indicated by the subscripts) found using thermodynamic steam-tables [11]. Again, the membrane gas humidifier was designed to ensure that $\phi_{g,hm,o} \approx 1$. This model of the mixer outlet relative humidity is physics based, depends only on measured variables, and does not contain parameters requiring identification.

The measurement inputs to the model, shown in Fig. 3, are the humidifier and bypass dry air mass flow rates and the gas temperatures and total pressures at the humidifier and mixer outlets. The measured and estimated mixer outlet relative humidities are compared in Fig. 4. The average estimation error was found to be 3.8% relative humidity with a standard deviation of 1.6% relative humidity. Of critical importance, the relative humidity estimator accurately captures the dynamic response throughout the experiment.

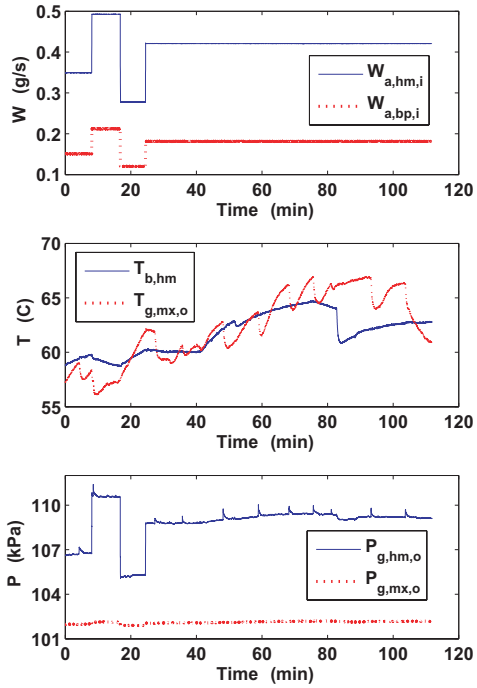

Fig. 3. Experimental Inputs to the relative humidity estimator.

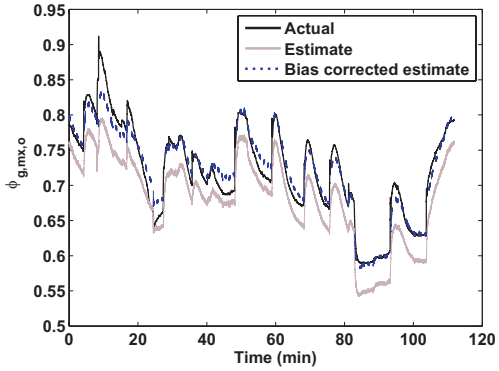

Fig. 4. Mixer outlet relative humidity estimation versus the measurement.

The relative humidity estimation contains a constant bias due to the use of different calibration standards for the mixer and humidifier outlet thermocouples versus the RTD probe embedded in the relative humidity sensor. By adding a constant 3.8% relative humidity to the estimation (equivalent to shifting the measured mixer outlet temperature by 1.2^{o}C), the steady-state estimation is improved, as shown in Fig. 4. The average estimation error for the bias corrected relative humidity estimation was then found to be 1.2% relative humidity with a standard deviation of 1.6%, which is less than sensor accuracy.

IV. SYSTEM THERMAL MODELING

The following general assumptions were made in developing the system thermal model due to the relatively narrow range of system operating temperatures (25-70^{o}C), pressures (close to atmospheric), and resulting thermal gradients. Caution should be taken when extending this model to operating conditions outside these ranges.

A1 There is no radiative heat loss from the control volumes. Heat loss to the surroundings is assumed to be a linear function of the difference in temperature as a result of natural convection alone.

A2 Under the range of operating temperatures and pressures considered, and assuming liquid water and air are incompressible, there is no change in mass stored within the control volumes.

A3 All constituents have constant specific heat and all gases behave ideally.

A4 Each control volume is homogenous and lumped parameter.

Each control volume is comprised of the material flowing through it, consisting of gases and/or liquid water, and the bulk materials that contain it, such as stainless or acrylic. For simplicity, the general model framework is provided here for the control volumes containing only gases. The temperature state, $T_{b,cv}$, represents the lumped temperature of the bulk materials which make up the control volume and the temperature state, $T_{g,cv}$, represents the temperature of the gases inside the control volume. Heat is transferred by forced convection from the bulk materials to the gases by $\hbar_{b2g,cv}A_{b2g,cv}(T_{b,cv} - T_{g,cv})$. Heat transfer from the bulk materials to the ambient occurs via natural convection and is represented by $\hbar_{b2amb,cv}A_{b2amb,cv}(T_{b,cv} - T_{amb})$. The heat transfer coefficients associated with forced convection are a function of mass flow rate, $\hbar_{b2g,cv} = \beta_{b2g,cv,1}W_{g,cv,i}^{\beta_{b2g,cv,2}}$, where as the heat transfer coefficients associated with natural convection are constant, $\hbar_{b2amb,cv} = \beta_{b2amb,cv}$.

Applying the conservation of energy, the resulting state equations are expressed for the bypass,

$$\frac{dT_{a,bp}}{dt} = \frac{1}{m_{bp}C_{bp}}\left[Q_{bp} + W_{a,bp,i}C_{p,a}(T_{a,bp,i} - T_{a,bp,o}) - \hbar_{b2amb,bp}A_{b2amb,bp}(T_{a,bp} - T_{amb})\right], \quad (3)$$

the water reservoir,

$$\begin{aligned}\frac{dT_{l,r}}{dt} =& \frac{1}{m_{l,r}C_{l,r}}\left[W_{l,fc,i}C_{p,l}(T_{l,fc,o} - T_{l,r,o})\right.\\ &+W_{l,wh,i}C_{p,l}(T_{l,hm,o} - T_{l,r,o})\\ &\left.-\hbar_{l2b,r}A_{l2b,r}(T_{l,r} - T_{b,r})\right],\\ \frac{dT_{b,r}}{dt} =& \frac{1}{m_{b,r}C_{b,r}}\left[\hbar_{l2b,r}A_{l2b,r}(T_{l,r} - T_{b,r})\right.\\ &\left.-\hbar_{b2amb,r}A_{b2amb,r}(T_{b,r} - T_{amb})\right], \quad (4a)\end{aligned}$$

the water heater,

$$\begin{aligned}\frac{dT_{l,wh}}{dt} =& \frac{1}{m_{l,wh}C_{l,wh}}\left[W_{l,hm,i}C_{p,l}(T_{l,r,o} - T_{l,hm,i})\right.\\ &\left.+\hbar_{b2l,wh}A_{b2l,wh}(T_{b,wh} - T_{l,wh})\right], \quad (5a)\\ \frac{dT_{b,wh}}{dt} =& \frac{1}{m_{b,wh}C_{b,wh}}\left[-\hbar_{b2l,wh}A_{b2l,wh}(T_{b,wh} - T_{l,wh})\right.\\ &\left.-\hbar_{b2amb,wh}A_{b2amb,wh}(T_{b,wh} - T_{amb}) + Q_{wh}\right], \quad (5b)\end{aligned}$$

the humidifier,

$$\frac{dT_{l,hm}}{dt} = \frac{1}{m_{l,hm}C_{l,hm}} [W_{l,hm,i}C_{p,l}(T_{l,hm,i} - T_{l,hm,o}) - \hbar_{l2amb,hm}A_{l2amb,hm}(T_{l,hm} - T_{amb}) - \hbar_{l2g,hm}A_{l2g,hm}(T_{l,hm} - T_{g,hm}) - W_{v,hm,o}C_{p,v}T_{g,hm,o}], \quad (6a)$$

$$\frac{dT_{g,hm}}{dt} = \frac{1}{m_{g,hm}C_{g,hm}} [W_{a,hm,i}C_{p,a}(T_{a,hm,i} - T_{g,hm,o}) + \hbar_{l2g,hm}A_{l2g,hm}(T_{l,hm} - T_{g,hm})], \quad (6b)$$

and the mixer,

$$\frac{dT_{g,mx}}{dt} = \frac{1}{m_{g,mx}C_{g,mx}} [(W_{a,hm,i}C_{p,a} + W_{v,hm,o}C_{p,v})(T_{g,hm,o} - T_{g,mx,o}) + W_{a,bp,i}C_{p,a}(T_{a,bp,o} - T_{g,mx,o}) + \hbar_{b2g,mx}A_{b2g,mx}(T_{b,mx} - T_{g,mx})], \quad (7a)$$

$$\frac{dT_{b,mx}}{dt} = \frac{1}{m_{b,mx}C_{b,mx}} [-\hbar_{b2g,mx}A_{b2g,mx}(T_{b,mx} - T_{g,mx}) - \hbar_{b2amb,mx}A_{b2amb,mx}(T_{b,mx} - T_{amb}) + Q_{mx}]. \quad (7b)$$

Note, the estimation of the water vapor mass flow rate, $W_{v,hm,o}$ in (6a) and (7a), is presented in (1). If the air supplied to the humidification system was not dry, and additional term could be added to account for the water vapor enthalpy supplied to the bypass and humidifier.

The constituent temperature state is considered either to be equal to the outlet temperature or the linear average between the inlet and outlet temperatures, depending upon the conditions of the control volume. After applying these relations, the measured control volume outlet conditions can be compared to the modeled estimates. These approximations are summarized by,

$$\begin{aligned} T_{a,bp,o} &= 2T_{bp} - T_{a,bp,i}, \\ T_{l,wh,o} &= 2T_{l,wh} - T_{l,r,o}, \\ T_{l,hm,o} &= 2T_{l,hm} - T_{l,hm,i}, \\ T_{l,r,o} &= T_{l,r}, \\ T_{g,hm,o} &= 2T_{g,hm} - T_{a,hm,i}, \\ T_{g,mx,o} &= T_{g,mx}, \end{aligned} \quad (8)$$

where the reservoir and the mixer are well mixed, implying that the lumped temperature is equal to the outlet temperature.

The model parameters, specified by employing material properties and known dimensions, are listed in Table I. For example, the mass of liquid water in the water heater was determined by measuring the internal volume and applying the average density of liquid water. The constant volume specific heats were calculated as mass weighted sums of the material components within the respective control volumes.

V. PARAMETER IDENTIFICATION

Prior to analyzing the system dynamics and designing controllers, the unknown heat transfer coefficients must be experimentally determined. These unknown parameters are tuned by minimizing the error between the measured and estimated outlet temperatures. Because the control volumes are cascaded, the outlet temperature measurement is used for parameter identification of each control volume, and then used as a measured input for subsequent control volumes. For example, the mixer identification utilizes measured bypass and humidifier air outlet temperatures rather than model estimates.

The cost function, $J = \frac{1}{n}\sum_{i=1}^{n}(\overline{T}_{cv,o} - \hat{T}_{cv,o})^2$, where n is the number of data points in the experiment, is minimized by adjusting the unknown parameter values using unconstrained nonlinear minimization (some heat transfer coefficients are nonlinear functions of constituent mass flow rates). Note, for the humidifier the sum of the squared liquid and gas estimation errors is minimized. Dynamic experiments were conducted to provide a rich data set for parameter identification, including multiple steps in the resistive heater power, along with steps in the total dry air mass flow supplied to the humidification system to mimic the air mass flow demand due to changes in the fuel cell electrical load.

The identified heat transfer coefficients are provided in Table II. As described in Section IV, these coefficients take on different functional forms depending upon the heat transfer process taking place. For all control volumes, constant heat transfer coefficients were considered for forced convection to reduce the number of identified parameters. Interestingly, this constant forced convection for heat transfer occurring between bulk materials and liquid water accurately captured the thermal response. Finally, due to the simplification of the bypass control volume from a two state to a single state system, the heat transfer loss from the control volume was assumed to be a linear function of flow rate (a combination of free and forced convection) of the form $\hbar_{bp} = \beta_{1,bp} + \beta_{2,bp}W_{a,bp,i}$. All of the identified parameters are close to or within the expected parameter ranges taken from [11] for natural and forced convection of liquids and gases.

TABLE I
MATERIAL PROPERTIES AND SYSTEM DESIGN PARAMETERS.

Mass (g)	**Specific Heat** (J/kg K)	**Area** (m^2)
m_{bp}=80	C_{bp}=460	A_{bp}=0.012
$m_{l,wh}$=50	$C_{l,wh}$=4180	$A_{b2l,wh}$=0.020
$m_{b,wh}$=780	$C_{b,wh}$=460	A_{wh}=0.028
$m_{l,hm}$=240	$C_{l,hm}$=4180	$A_{l2amb,hm}$=0.202
$m_{g,hm}$=18	$C_{g,hm}$=983	$A_{l2g,hm}$=0.03
$m_{g,mx}$=10	$C_{g,mx}$=863	$A_{b2g,mx}$=0.009
$m_{b,mx}$=745	$C_{b,mx}$=460	A_{mx}=0.012
$m_{l,r}$=2800	$C_{l,r}$=4180	$A_{l2b,r}$=0.075
$m_{b,r}$=1540	$C_{b,r}$=957	$A_{b2amb,r}$=0.087
	$C_{p,a}$=1004	
	$C_{p,v}$=1872	
	$C_{p,l}$=4180	

TABLE II

EXPERIMENTALLY IDENTIFIED HEAT TRANSFER COEFFICIENTS.

Expected Range	**Identified Value** (W/m^2K)
$50-20000$	$\hbar_{b2l,wh}$=139.8 and $\hbar_{l2b,r}$=167.5
$50-1000$	$\hbar_{b2amb,wh}$=0 and $\hbar_{l2amb,hm}$=22.5 $\hbar_{b2amb,r}$=80.0
$5-250$	$\hbar_{bp}$=10.8-21822$W_{a,bp,i}$
$5-25$	$\hbar_{b2amb,mx}$=25.8
$25-250$	$\hbar_{b2g,mx}$=2819$W_a^{0.54}$
$25-20000$	$\hbar_{l2a,hm}$=41029$W_{a,hm,i}^{0.95}$

VI. EXPERIMENTAL VALIDATION

For model validation, the control volumes were combined such that the estimation of the temperature leaving one control volume is treated as an input to subsequent control volumes. An experiment, different than that used for parameter identification, was then conducted and compared to the temperature measurements for validating the thermal model.

The estimated bypass air outlet temperature is compared with the measurement in Fig. 5. For changes in the air mass flow rate and the bypass heater, the model captures the response time. However, there is an offset in the steady-state temperature estimation throughout most of the experiment, due to an overestimation of the heat loss from the control volume to the ambient. Linearization of the bypass state equation, has shown that the bypass pole location is most sensitive to air flow, and not the heat transfer coefficient. As a result, this steady-state error will have little impact on the resulting controller design. The average estimation error was 2.8^{o}C with a standard deviation of 1.4^{o}C.

The estimated water reservoir outlet temperature is compared with the measurement in Fig. 6. The reservoir system is driven by the estimate of the liquid water temperature leaving the humidifier and represents a significant thermal lag in the water circulation system due to the relatively large stored water mass. The reservoir model captures both the slow response following the humidifier dynamics as well as the steady-state temperature. The average estimation error was 0.3^{o}C with a standard deviation of 0.3^{o}C.

The estimated water heater outlet temperature is compared with the measurement in Fig. 7. The water heater model captures the slow response due to changes in the heater as well as the steady-state temperature. The average estimation error was 0.5^{o}C with a standard deviation of 0.4^{o}C.

The estimated air and liquid water temperatures leaving the humidifier are compared with the measurements in Fig. 8. The humidifier air outlet temperature estimation error increases when the system is cooling down. This offset is thought to be the result of neglecting the condensation of water on the air side of the humidifier, a complex process neglected here. However, the air temperature is well approximated during warm-up and captures the correct dynamic response throughout the experiment. The response of the liquid water is also well approximated throughout the experiment. The average estimation errors were 1.3^{o}C and 0.7^{o}C with standard deviations of 1.1^{o}C and 0.5^{o}C, for the air and liquid water respectively.

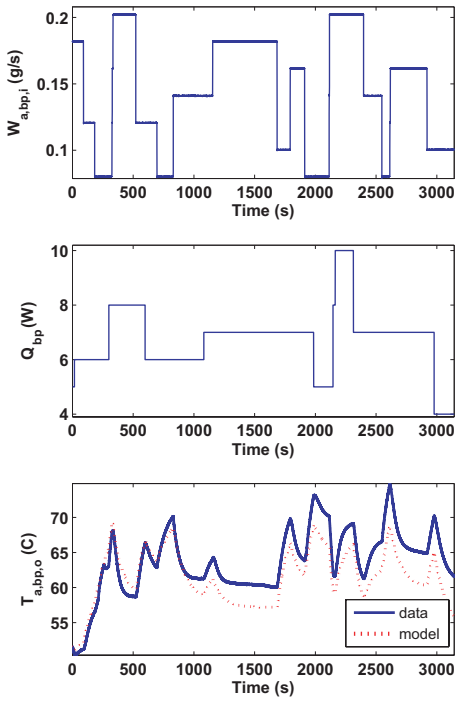

Fig. 5. Bypass experimental validation results.

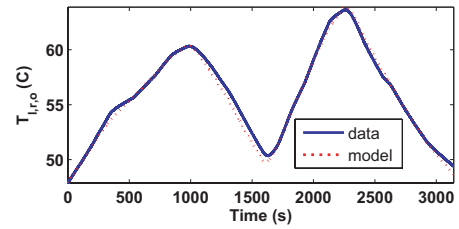

Fig. 6. Reservoir experimental validation results.

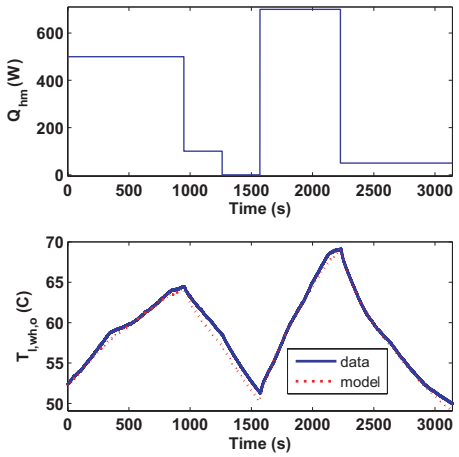

Fig. 7. Water heater experimental validation results.

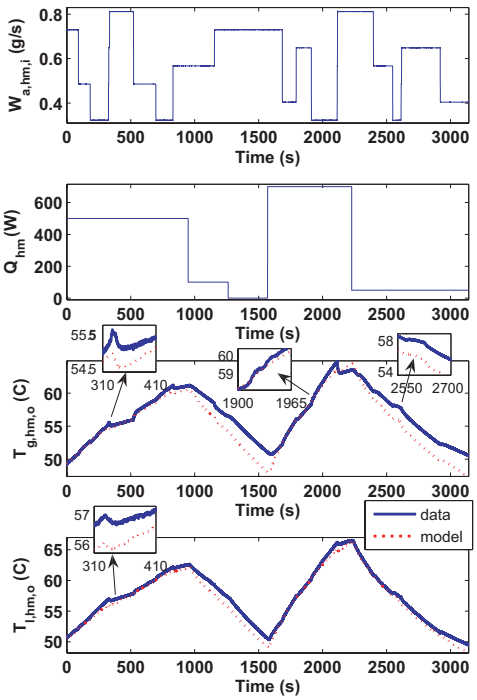

Fig. 8. Humidifier experimental validation results.

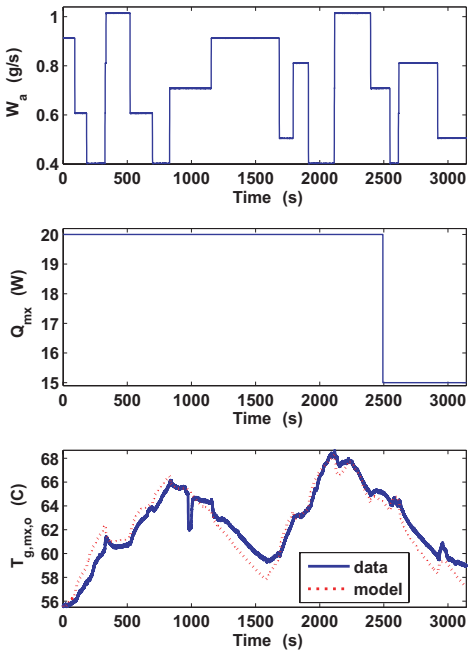

Fig. 9. Mixer experimental validation results.

The estimated mixer air outlet temperature is compared with the measurement in Fig. 9. The mixer response to changes in air mass flow rate or mixer heat are well captured throughout the experiment. An improvement in the humidifier estimation during the cool down portion of the experiment may improve the mixer estimation during this period. Note, at approximately 1000 seconds, the measured mixer outlet temperature momentarily decreases dramatically. The cause of this rapid decrease and then increase in temperature is unknown but was an isolated event that could not be reproduced. The average estimation error was 0.8^oC with a standard deviation of 0.5^oC.

VII. CONCLUSIONS

An apparatus was devised to regulate the temperature and relative humidity of reactant gases supplied to a fuel cell. For controller development, a physics based, control oriented model of the thermal and humidity dynamics of this membrane-type humidification system was developed and experimentally validated. The humidity dynamics are accurately estimated under a range of operating conditions using a simple nonlinear output equation. The thermal dynamics of the various control volumes, related time constants, and impact of the operating conditions on the thermal response are modeled to generate an accurate approximation of system temperatures. Future work will employ this humidification system model to design and implement controllers that regulate the exhaust relative humidity and temperature despite disturbances in air mass flow rate.

REFERENCES

[1] E. Mueller, A. Stefanopoulou, and L. Guzzella, "Optimal power control of hybrid fuel cell systems for an accelerated system warm-up," *IEEE Transactions on Control Systems Technology*, vol. 15, no. 2, pp. 290–305, 2007.

[2] D. McKay, J. Siegel, W. Ott, and A. Stefanopoulou, "Parameterization and prediction of temporal fuel cell voltage behavior during flooding and drying conditions," *Journal of Power Sources*, vol. 178, no. 1, pp. 207–222, 2008.

[3] A. Karnik, A. Stefanopoulou, and J. Sun, "Water equilibria and management using a two-volume model of a polymer electrolyte fuel cell," *Journal of Power Sources*, vol. 164, pp. 590–605, 2007.

[4] A. Love, S. Middleman, and A. Hochberg, "The dynamics of bubblers as vapor delivery systems," *Journal of Crystal Growth*, vol. 129, pp. 119–133, 1993.

[5] K. Choi, D. Park, Y. Rho, Y. Kho, and T. Lee, "A study of the internal humidification of an integrated pemfc stack," *Journal of Power Sources*, vol. 74, pp. 146–150, 1998.

[6] D. Staschewski, "Internal humidifying of pem fuel cells," *International Journal of Hydrogen Energy*, vol. 21, no. 5, 1996.

[7] D. Chen and H. Peng, "A thermodynamic model of membrane humidifiers for pem fuel cell humidification control," *Transaction of the ASME, Journal of Dynamic Systems, Measurement and Control*, vol. 127, pp. 424–432, 2005.

[8] W. Wheat, B. Clingerman, and M. Hortop, "Electronic by-pass control of gas around the humidifier to the fuel cell," U.S. Patent number 6884534, April 2005.

[9] E. Cortona, C. Onder, and L. Guzzella, "Engine thermomanagement with electrical components for fuel consumption reduction," *IMechE Int. Journal of Engine Research*, vol. 3, no. 3, pp. 157–170, 2002.

[10] P. Setlur, J. Wagner, D. Dawson, and E. Marotta, "An advanced engine thermal management system: Nonlinear control and test," *IEEE/ASME Transactions on Mechatronics*, vol. 10, no. 2, 2005.

[11] Sonntag, Borgnakke, and V. Wylen, *Fundamentals of Thermodynamics*. John Wiley and Sons, 2003.